

Magneto-Optical Properties of Terbium Aluminum Garnet at Liquid-Helium Temperatures

WARREN DESORBO

General Electric Research and Development Center, Schenectady, New York

(Received 28 December 1966)

The Verdet constant of a terbium aluminum garnet crystal (flat disk) has been measured at liquid-helium temperatures in the visible spectral range. Values appropriate to a sample with no demagnetizing field have been calculated from internal fields of the specimen rather than the external field, using standard demagnetization corrections and volume-susceptibility data. Photographs taken of the crystal in field values H in the vicinity of a 180° rotation illustrate the significance of demagnetizing fields. From such observations the distribution of internal magnetic fields in nonellipsoidal specimens can be mapped out. These new Verdet-constant data serve to verify further the proportionality of Verdet constant and magnetic susceptibility postulated by Van Vleck and Hebb. The onset of magnetic saturation at relatively low fields is due to the low temperatures of the measurement and to the large splitting factor associated with the ground state of Tb^{3+} . The frequency dependence of the Verdet constant is in satisfactory agreement with the simple theory proposed by Rosenfeld.

INTRODUCTION

RECENTLY, Rubinstein, Van Uitert, and Grodkiewicz¹ have shown that terbium aluminum garnet (TbAlG) has, in the visible spectral range, a relatively high Verdet constant and a low optical absorption. These properties, they remark, make it useful in optical Faraday-effect devices. Their measurements on the Verdet constant were carried out at room temperature and at 77°K . Since materials of this nature have also proven useful in instrumentation making use of the Faraday effect at liquid-helium temperatures, it was deemed important to extend the Verdet-constant measurements of terbium aluminum garnet to these lower temperatures. More specifically we refer to instrumentation used in studies on the intermediate state of superconductors (e.g., see Ref. 2). A higher Verdet constant for this application is desirable for both increased resolution and for lower-limit field detection. One purpose of the work, then, was to compare the Verdet constant at liquid-helium temperatures with that obtained in materials now being used, primarily cerous phosphate glass.^{2,3} Secondly, such measurements might serve to verify further the proportionality of Verdet constant and magnetic susceptibility postulated by Van Vleck and Hebb.⁴ Lastly, rotation measurements may allow one to visualize the distribution of internal fields in an irregularly shaped specimen.

EXPERIMENTAL

The garnet sample (flat disk) was cut from a crystal kindly supplied us by Rubinstein. Details of its preparation are presented in Ref. 1. The sample used in the experiment was ground and polished to a final thickness of 6.86×10^{-2} cm. The single-crystal x-ray density is 6.06 g/cc calculated from cubic-lattice param-

eter, $a_0 = 12.077 \pm 0.003 \text{ \AA}$ obtained by L. M. Osika of our laboratory. The plane of the crystal had a (110) orientation; therefore, the highest-order reflecting plane, namely $10 \cdot 10 \cdot 0$, was used to measure the lattice parameter.

The Faraday rotation measurements from which the Verdet constants were derived were made with the apparatus used in studying the intermediate state of superconductors already described.² The monochromatic light was provided by a Farrand grating monochromator. Minimum light transmission observations to determine the angle of rotation for a given field were accomplished by naked eye and by the use of a Welch Densichron (W. M. Welch Manufacturing Co., Chicago, Illinois). In the experimental setup, the light is transmitted through the sample and reflected back by a silver film ($\sim 0.2\mu$ thick) deposited on the underside. The rotated light then passes through a half-silvered mirror tilted 45° with respect to the beam and reaches the analyzer.² The polarizer is set so that for 0° , 180° , 360° , etc. rotations of the light, the electric vector of the light is parallel to the half-silvered surface. However, for intermediate rotations, a minor difficulty is encountered owing to the fact that the half-silvered mirror introduces both rotation and ellipticity to the light passing through it. As a result, direct measurement for small rotations of light yield an apparent rotation after passage through the mirror that is 27% larger than the actual rotation. This correction is made to all the appropriate data. In evaluating the Verdet constant, the effective thickness of the specimen is twice the actual thickness.

RESULTS AND DISCUSSION

A. Verdet Constant

Figure 1 shows the observed rotation of the polarization plane of monochromatic light for different wavelengths in the visible range at 1.45°K as a function of applied magnetic field. The values of the Verdet con-

¹ C. B. Rubinstein, L. G. Van Uitert, and W. H. Grodkiewicz, *J. Appl. Phys.* **35**, 3069 (1964).

² W. DeSorbo and W. A. Healy, *Cryogenics* **4**, 257 (1964).

³ P. B. Alers, *Phys. Rev.* **116**, 1483 (1959).

⁴ J. H. Van Vleck and M. H. Hebb, *Phys. Rev.* **46**, 17 (1934).

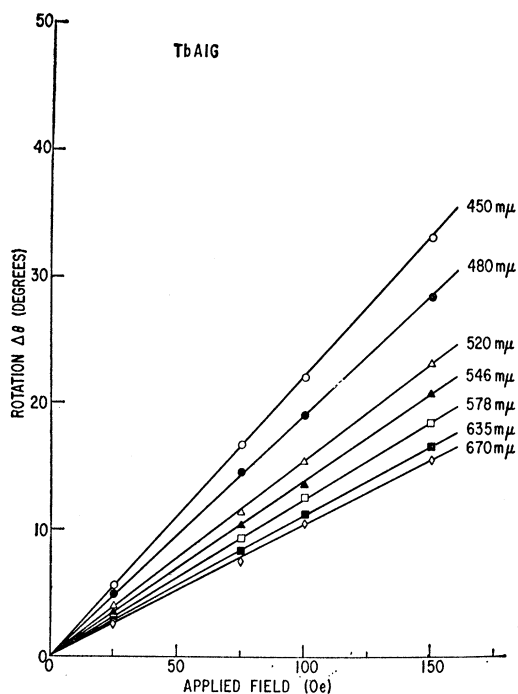


FIG. 1. The rotation in degrees of the plane of polarization of several wavelengths of light in the visible range as a function of applied transverse magnetic field for terbium aluminum garnet ($T=1.45^\circ\text{K}$). "Effective" light path thickness equals approximately 0.14 cm.

stant corresponding to different wavelengths are presented in Table I at the two temperatures investigated, 4.22°K and 1.45°K , in units of $\text{min}/\text{Oe cm}$. The uncorrected values, $V_{\text{uncor.}}$, are those derived from the rotation based on the value of the applied external field. The corrected values, $V_{\text{cor.}}$, are those appropriate to a sample with no demagnetizing field and are calculated from the internal field of the specimen rather than the external field (see Sec. B below). The values of the Verdet constant of cerous phosphate glass have been reported only for the wavelength $546 \text{ m}\mu$ at liquid-helium temperatures.^{2,3} A comparison of these results with those reported here show that the Verdet constant of terbium aluminum garnet is larger by at least an order of magnitude for this wavelength in this temperature range.

TABLE I. Measured Verdet constant of terbium aluminum garnet ($3\text{Tb}_2\text{O}_3 \cdot 5\text{Al}_2\text{O}_3$) in the liquid-helium temperature range.

Wave-length ($\text{m}\mu$)	Verdet constant ($\text{min}/\text{Oe cm}$)			
	4.22°K		1.45°K	
	$V_{\text{uncor.}}$	$V_{\text{cor.}}$	$V_{\text{uncor.}}$	$V_{\text{cor.}}$
450	-65.25	-102.16	-97.10	-200.95
480	-53.30	-83.45	-83.37	-172.52
520	-41.39	-64.80	-67.31	-139.28
546	-37.26	-58.35	-60.44	-125.07
578	-34.34	-53.77	-53.77	-111.27
635	-30.91	-48.39	-47.10	-97.47
670	-30.04	-47.04	-45.15	-93.42

As expected, the data show large increases in the Verdet constant with decrease in temperature. In Fig. 2 the results obtained at the liquid-helium temperatures are compared with those obtained by Rubinstein *et al.*¹ at liquid nitrogen and room temperatures. Van Vleck and Hebb⁴ have shown that in rare-earth compounds the Verdet constant should exhibit the same temperature dependence as the magnetic susceptibility χ . That this agreement exists in aluminum terbium garnet is quite evident when the low temperature susceptibility data of Wolf *et al.*⁵ are compared with the data of this report. At approximately 1.5°K the susceptibility data exhibit a maximum. The decrease in value below this temperature has been interpreted as due to the onset of antiferromagnetic ordering. Since the Verdet-con-

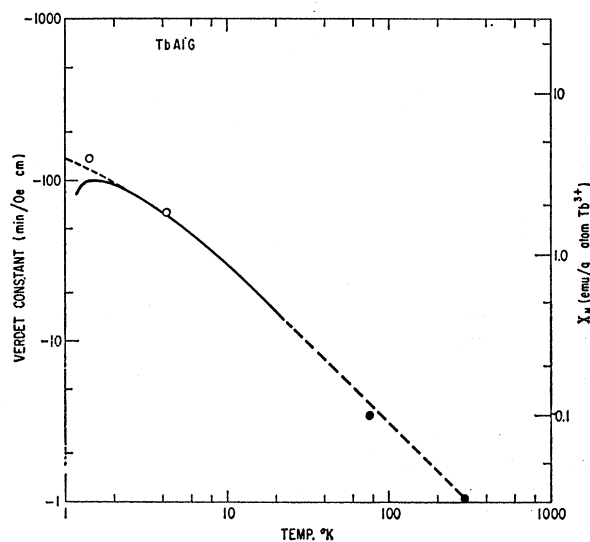


FIG. 2. The Verdet constant as a function of temperature showing both the results of Rubinstein *et al.* (Ref. 1) (●), and those of this work (○) for the wavelength $\lambda=520 \text{ m}\mu$. The solid curve gives the magnetic susceptibility data of Wolf *et al.* (Ref. 5). The dashed curve is a Curie-Weiss law with a Curie constant of 9.1 and T_c of -1.3°K . This curve is intended to give a reasonable extrapolation to high temperatures of the low-temperature susceptibility data.

stant measurement at the lowest temperature reported here (i.e., 1.45°K) is near this value, no significant decrease in Verdet constant is observed. Presumably, below this temperature region large decreases in V can be expected. The dashed line on Fig. 2 shows the best Curie-Weiss fit to the data of Wolf *et al.*,⁵ i.e., $\chi_M = 9.1/(T+1.3)$.

At higher fields one should expect a deviation from linearity in the plot of rotation versus field owing to the onset of magnetic saturation. This phenomenon, first described by Becquerel and de Haas⁶ is shown in Fig. 3. The onset is at relatively low fields owing to the low

⁵ W. P. Wolf, M. Ball, M. T. Hutchings, M. J. M. Leask, and A. F. G. Wyatt, *J. Phys. Soc. (Japan)* **17**, Suppl. BI (1962).

⁶ J. Becquerel and W. J. de Haas, *Z. Physik* **52**, 678 (1928).

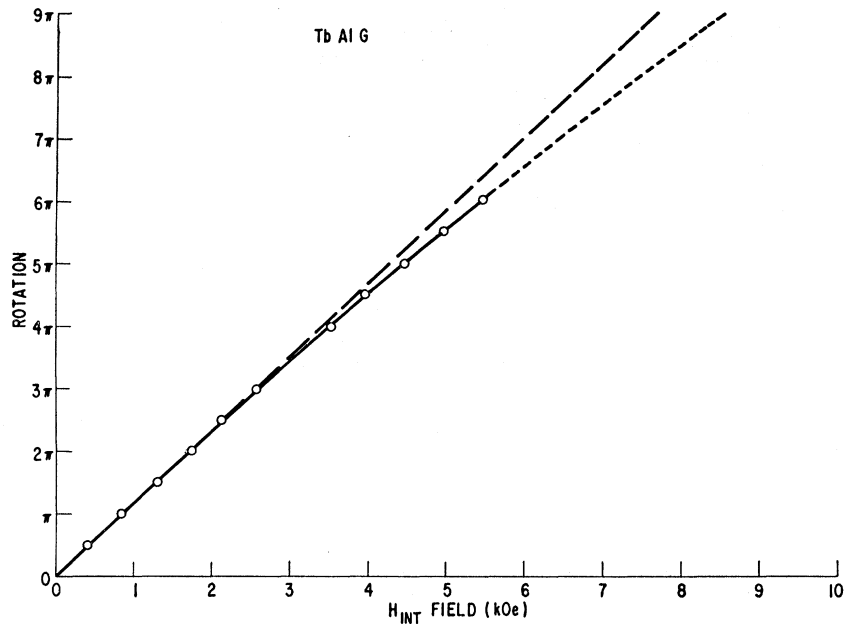


FIG. 3. The rotation of the plane of polarized light ($\lambda=546 \text{ m}\mu$) as a function of the internal field of the specimen ($T=1.45^\circ\text{K}$).

temperature of measurement and the large splitting factor associated with the ground state of Tb^{3+} .

Lastly, we may compare the frequency dependence of the Verdet constant with the simple theory proposed by Rosenfeld⁷ wherein the paramagnetic temperature-dependent Verdet constant is given by the proportionality,

$$V \propto F(\mu H/kT)[1/(\nu^2 - \nu_0^2)], \quad (1)$$

where the $F(\mu H/kT)$ describes the relative occupancy of various multiplet levels and ν and ν_0 are the frequency of measurement and frequency of the main resonance giving rise to the effect. Figure 4 shows a plot of the reciprocal of the Verdet constant against the reciprocal square of wavelength. The straight lines on this graph indicate that Eq. (1) is a good description of the frequency dependence if λ_0 is assumed to be $376 \pm 5 \text{ m}\mu$ or $1/\lambda_0 = 26\,500 \pm 400 \text{ cm}^{-1}$. This value compares favorably with the transition ${}^7F_6 - {}^5D_3$ of $26\,200 \text{ cm}^{-1}$, observed by Thomas *et al.* in the absorption spectrum of Tb^{3+} in LaCl_3 .⁸ This particular transition is a prominent one and the transition frequencies are split by the magnetic field.

B. Demagnetizing Fields

By the standard demagnetizing correction, the relation between the internal field and external field is

$$H_{\text{internal}} = H_{\text{applied}} / [1 + (4\pi - 2N_1)\chi_v], \quad (2)$$

where χ_v is the volume susceptibility and N_1 is the demagnetization factor in the plane of the disk. From the

data of Wolf *et al.*,⁵ we take the volume susceptibilities to be 0.046₅ and 0.087₉ at 4.22 and 1.45°K, respectively. Treating the disk as an oblate spheroid with a dimensional ratio of ten to one, the value of N_1 is approximately 0.2.⁹ As may be seen from Eq. (2), the exact value is unimportant. With these assumptions the internal field by Eq. (1), is 0.63₉ and 0.48₂ of the value of the applied field at 4.22 and 1.45°K, respectively.

Demagnetizing fields are uniform only for ellipsoids. Tools have not been available for mapping out these fields in nonellipsoidal specimens. The significance of these demagnetization fields may be better appreciated

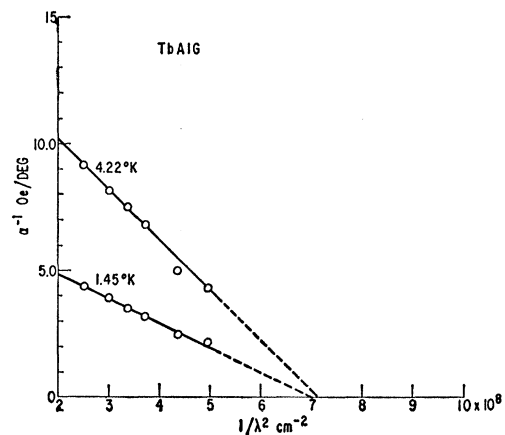


FIG. 4. The inverse Verdet constant α^{-1} as a function of $1/\lambda^2$ where λ is the wavelength in the visible region for each temperature, 4.22 and 1.45°K, respectively. $\lambda_0 = 376 \pm 5 \text{ m}\mu$.

⁷ L. Rosenfeld, *Z. Physik* **57**, 835 (1929).

⁸ K. S. Thomas, S. Singh, and G. H. Dieke, *J. Chem. Phys.* **38**, 2180 (1963).

⁹ R. M. Bozorth, *Ferromagnetism* (D. Van Nostrand Company, Inc., New York, 1959), p. 846.

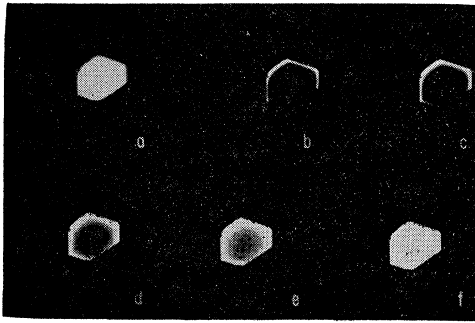


FIG. 5. Photographs of the process of light extinction caused by a 180° rotation of $546\text{ m}\mu$ at 1.45°K . In zero applied field, the polarizer and analyzer were crossed. The applied fields are (a) 1095 Oe, (b) 1336 Oe, (c) 1383 Oe, (d) 1418 Oe, (e) 1458 Oe, and (f) 1497 Oe. The crystal is an irregular, roughly hexagonal flat plate—maximum dimension 0.9 cm, minimum 0.6 cm, and thickness 6.9×10^{-2} cm.

by examining the photos in Fig. 5 at field values H in the vicinity of a rotation of 180° . In Fig. 5(a), the sample appears bright except for a narrow black rim present along its periphery. The field profile for this case, idealized for a cylindrical flat specimen, corresponds to the situation presented by curve a in Fig. 6. That is, the internal field has a value corresponding to a rotation of 180° only near the edge of the sample. Fig. 5(b) represents the case at a slightly higher field,

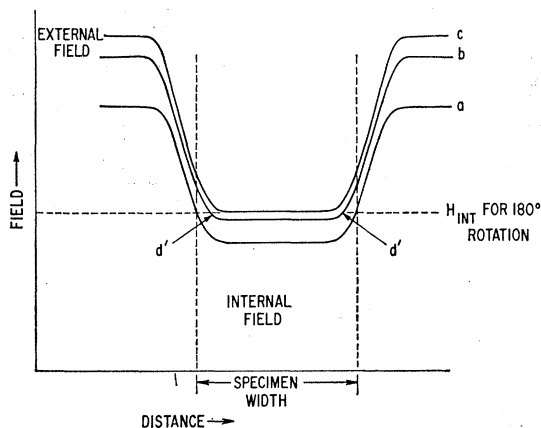


FIG. 6. A diagrammatic sketch showing the idealized and approximate relationship of the applied magnetic field to the internal field of the garnet (assumed to be a cylindrical flat plate) in the vicinity of the internal field corresponding to a 180° rotation of the impinging monochromatic light.

corresponding to curve b of Fig. 6. In this situation, the internal field near the line described by the circle $d'-d'$ has a value corresponding to a 180° rotation of the light. Hence, there is a dark rim in this region of the crystal. Photo (c) shows the result at a still slightly higher field where a large area in the center of the specimen is at the value of the internal field corresponding to a 180° rotation (curve c of Fig. 6). The outer edge of the specimen is at higher internal fields and therefore still appears light. Photos (d), (e), and (f) show the demagnetization field at successively higher applied field values. We may compare these observations with the simple demagnetization theory by assuming that the internal field in the bulk of the specimen is given by Eq. (2) and that the applied field for extinction in the body of the crystal is 1380 ± 25 Oe. By the calculation of the paragraph above, we estimate the internal field to be 666 ± 12 Oe for extinction. To make a rough estimate of the condition for extinction at the edge of the crystal we note from symmetry that the normal component of the demagnetizing field at the edge of a uniformly magnetized semi-infinite sheet is just one half of its value in the bulk of the sheet. The internal field, in this, approximation would be 0.74_1 of the applied field, and, hence, the applied field for extinction at the edge would be estimated as $666/0.74_1$ or about 900 ± 20 Oe. Since the material is not uniformly magnetized, owing to the spatial variation in internal fields, but is more magnetized at the outer edges, the demagnetizing field would be greater than that derived above for uniform magnetization. Therefore, we would expect the ratio of internal field to external field to be somewhat less than the value of 0.74 calculated above for uniform magnetization. From the observation, reproduced in Fig. 5(a), that an external field of 1095 Oe just produces some edge extinction, we observe this factor to be $666/1095$ or 0.60_6 . By observations such as these, one can map out the distribution of internal magnetic fields in nonellipsoidal specimens—a quantity that is not amenable to analysis.

ACKNOWLEDGMENTS

The author wishes to thank C. P. Bean for helpful conversations. He is indebted to C. B. Rubinstein for making the crystal available and to A. G. Pincus for his interest in this work. The writer also thanks W. A. Healy for capable assistance in the experimental work.

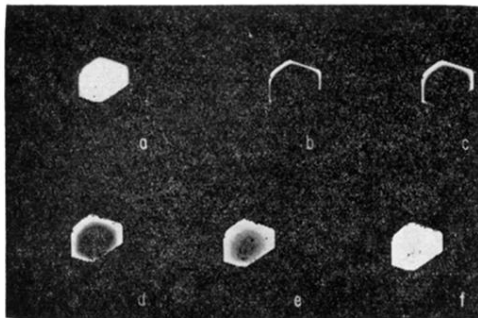


FIG. 5. Photographs of the process of light extinction caused by a 180° rotation of $546\text{ m}\mu$ at 1.45°K . In zero applied field, the polarizer and analyzer were crossed. The applied fields are (a) 1095 Oe, (b) 1336 Oe, (c) 1383 Oe, (d) 1418 Oe, (e) 1458 Oe, and (f) 1497 Oe. The crystal is an irregular, roughly hexagonal flat plate—maximum dimension 0.9 cm, minimum 0.6 cm, and thickness 6.9×10^{-2} cm.